Nuclear Instruments and Methods in Physics Research A 702 (2013) 29–33

Contents lists available at SciVerse ScienceDirect

Nuclear Instruments and Methods in Physics Research A

journal homepage: www.elsevier.com/locate/nima

What approach to brain partial volume correction is best for PET/MRI?

B.F. Hutton [a,*], B.A. Thomas [a], K. Erlandsson [a], A. Bousse [a], A. Reilhac-Laborde [b], D. Kazantsev [c], S. Pedemonte [c], K. Vunckx [d], S.R. Arridge [c], S. Ourselin [c]

[a] Institute of Nuclear Medicine, UCL, 235 Euston Road, London NW1 2BU, UK
[b] Australian Nuclear Science and Technology Organisation, Illawarra Road, Sydney, Australia
[c] Centre for Medical Image Computing, UCL, Malet Place Engineering, London WC1E 6BT, UK
[d] Department of Nuclear Medicine, Katholieke Universiteit Leuven, B-3000 Leuven, Belgium

ARTICLE INFO

Article history:
Received 8 June 2012
Received in revised form
26 July 2012
Accepted 30 July 2012
Available online 10 August 2012

Keywords:
Positron emission tomography
Magnetic resonance imaging
Partial volume correction
Anatomical priors

ABSTRACT

Many partial volume correction approaches make use of anatomical information, readily available in PET/MRI systems but it is not clear what approach is best. Seven novel approaches to partial volume correction were evaluated, including several post-reconstruction methods and several reconstruction methods that incorporate anatomical information. These were compared with an MRI-independent approach (reblurred van Cittert) and uncorrected data. Monte Carlo PET data were generated for activity distributions representing both ^{18}F FDG and amyloid tracer uptake. Post-reconstruction methods provided the best recovery with ideal segmentation but were particularly sensitive to mis-registration. Alternative approaches performed better in maintaining lesion contrast (unseen in MRI) with good noise control. These were also relatively insensitive to mis-registration errors. The choice of method will depend on the specific application and reliability of segmentation and registration algorithms.

1. Introduction

Correction for the influence of spatial resolution in emission tomography (usually referred to as partial volume (PV) effects) remains a challenge despite the availability of a wide range of suggested approaches [1]. Several of the widely used approaches make direct use of an anatomical MRI study to enable correction between identified compartments (e.g. grey matter, white matter and CSF). Alternatively in reconstruction, resolution can be modelled and anatomical information incorporated as a prior, aiming to reduce bias, while controlling noise in the reconstructed data. There is little published in cross-comparison of recently developed methods, especially between post-reconstruction approaches and the much-favoured approaches that tackle the problem during reconstruction. The availability of PET/MRI greatly improves the logistics of acquiring well-registered PET and MRI data in individuals and so should encourage routine PV correction. It is not clear, however, which approach should be adopted to optimise quality and quantitative accuracy of the reconstructed images. In this paper we present a preliminary comparison of a range of recently developed algorithms to better inform choice of approach for PET/MRI brain studies.

2. Methods

2.1. Simulation studies

We used Monte Carlo simulation [2] to generate realistic PET acquisition data for a Siemens HR+ PET camera. The activity distribution was determined by first segmenting a patient MRI study (Freesurfer) and allocating values to segmented regions based on realistic clinical distributions of ^{18}F–FDG and ^{18}F labelled amyloid tracers. Most regions were allocated uniform activity; however, variability was introduced in some regions to reflect departures from the assumption that all regions could be considered uniform. This included cold lesions on the FDG study (Fig. 1(a)) and regions where regional uptake was heterogeneous on the amyloid studies. Ten noise realisations were generated for counts consistent with clinical practice; in addition high count data were generated for each phantom. In addition to the perfectly registered MRI data (and associated attenuation map), mis-registered MRI studies were obtained using rigid transformation; this was used to evaluate sensitivity to mis-registration

* Corresponding author. Tel.: +44 2034470531; fax: +44 2034470528.
E-mail addresses: brian.hutton@uclh.nhs.uk (B.F. Hutton), benjamin.thomas2@uclh.nhs.uk (B.A. Thomas), kjell.erlandsson@uclh.nhs.uk (K. Erlandsson), alexandre.bousse@uclh.nhs.uk (A. Bousse), anthonin@ansto.gov.au (A. Reilhac-Laborde), d.kazantsev@cs.ucl.ac.uk (D. Kazantsev), s.pedemonte@cs.ucl.ac.uk (S. Pedemonte), kathleen.vunckx@UZleuven.be (K. Vunckx), s.arridge@cs.ucl.ac.uk (S.R. Arridge), s.ourselin@cs.ucl.ac.uk (S. Ourselin).

0168-9002/$ - see front matter © 2012 Elsevier B.V. All rights reserved.
http://dx.doi.org/10.1016/j.nima.2012.07.059

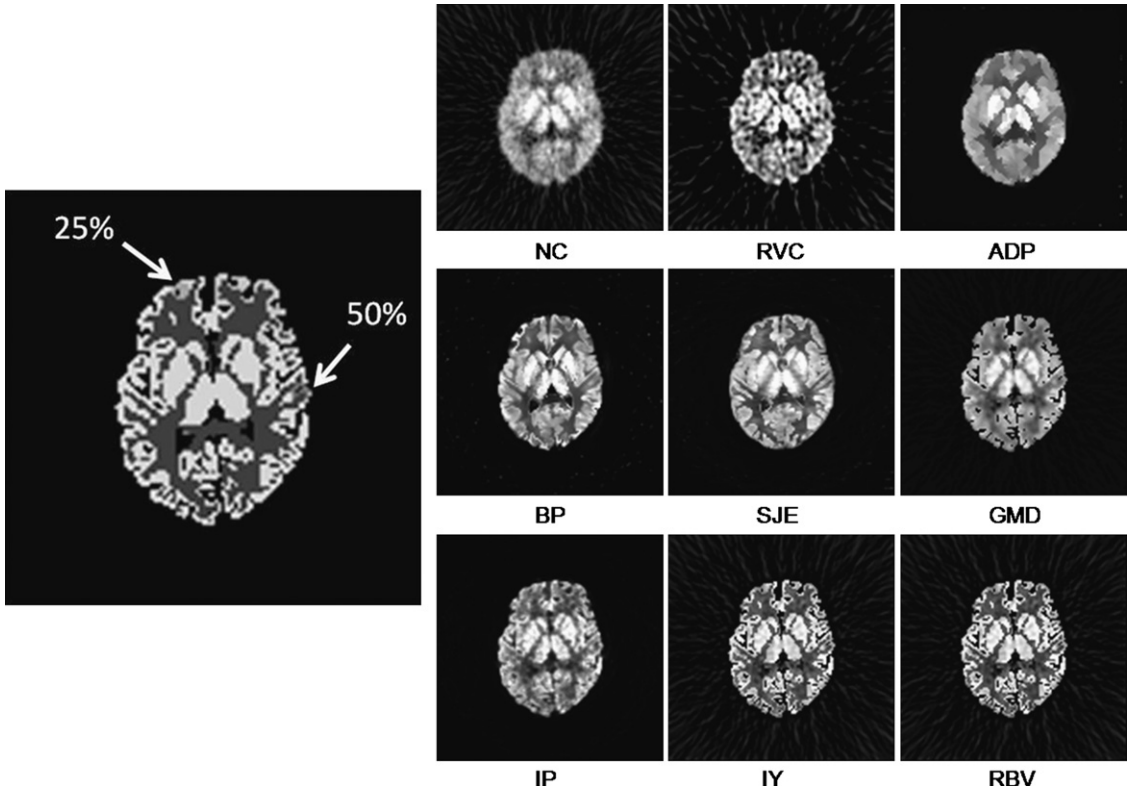

Fig. 1. (a) Sample transaxial slice of the ^{18}F–FDG distribution used for simulation. The locations of two cold lesions are indicated, with cortical activity reduced by 25% and 50%. (b) Sample transaxial slices for ^{18}F–FDG simulations, corrected for partial volume using various approaches. NC: no correction, RVC: reblurred van Cittert, ADP: anisotropic diffusion prior, BP: modified Bowsher prior, SJE: semi-parametric joint entropy, GMD: Gaussian mixture deconvolution, IP: iterative projection, IY: iterative Yang, and RBV: region based voxel-wise.

errors. Studies for assessing post-reconstruction PV correction algorithms were reconstructed using filtered back projection, post-smoothed with a Gaussian (4 mm full-width at half-maximum); the reconstructed impulse response function was estimated by determining the Gaussian function that, when convolved with the original simulated object, best matched the reconstruction. The simulated acquisition data were also reconstructed with alternative algorithms that incorporate MRI without the need for segmentation as described below. In this case point source projections were used to establish an appropriate resolution model.

2.2. PV correction methods

Eight alternative approaches to PV correction were evaluated and compared with uncorrected data:

i) Region-based voxel-wise (RBV) correction [3]—this approach combines the GTM method [4], which permits regional mean values for the segmented regions to be determined, with extension of the voxel-based Yang approach [5], which simultaneously updates multiple regions on a voxel by voxel basis rather than treating regions separately.
ii) Iterative Yang (IY) correction—this algorithm, suggested in Ref. [1] uses the Yang approach [5] in an iterative loop where an estimate of regional mean values is updated, based on current values; five iterations of the algorithm appears to be sufficient to reach a stable solution. The resultant algorithm is therefore very efficient.
iii) Iterative projection (IP) correction [6]—a further variation on the IY approach performs the correction step in the projection space; this method accounts for spatial variation in resolution via the projector rather than estimating a reconstructed impulse response function and so is particularly attractive for SPECT studies.
iv) Gaussian mixture model based deconvolution (GMD) [7]—this novel approach assumes that the activity distribution in each region can be approximated by a Gaussian mixture, with uncertainty defined both by a segmented MRI and 'hidden' underlying activity classes represented by a Markov random field. It extends on methods that use direct iterative deconvolution [8].
v) Use of the Bowsher prior (BP)—this modified implementation [9] selects a neighbourhood based on the most similar MRI values (13 of 80 neighbours), within which a relative difference potential function is applied, preserving anatomical boundaries defined by the MRI without the need for specific segmentation.
vi) Anistropic diffusion filtering (ADP) [10]—this attempts to iteratively optimise edge preservation while suppressing noise in combination with a MLEM reconstruction; the aim of the two-stage iteration is to maintain PET contrast that is absent in the MRI.
vii) Semi-parametric joint entropy reconstruction (SJE) [11]—based on an assumption that both MRI and PET are derived from a distribution of hidden variables, this algorithm uses a novel probabilistic framework for reconstruction that attempts to estimate the activity distribution from the PET raw data, with a penalty term defined as the joint entropy of the MR image (described as a Gaussian mixture) and the activity (described with a non-parametric model).
viii) Reblurred van Cittert (RVC) [8]—for reference we have included a method that is not dependent on anatomical information but performs direct iterative deconvolution. Results were also compared with uncorrected data (NC).

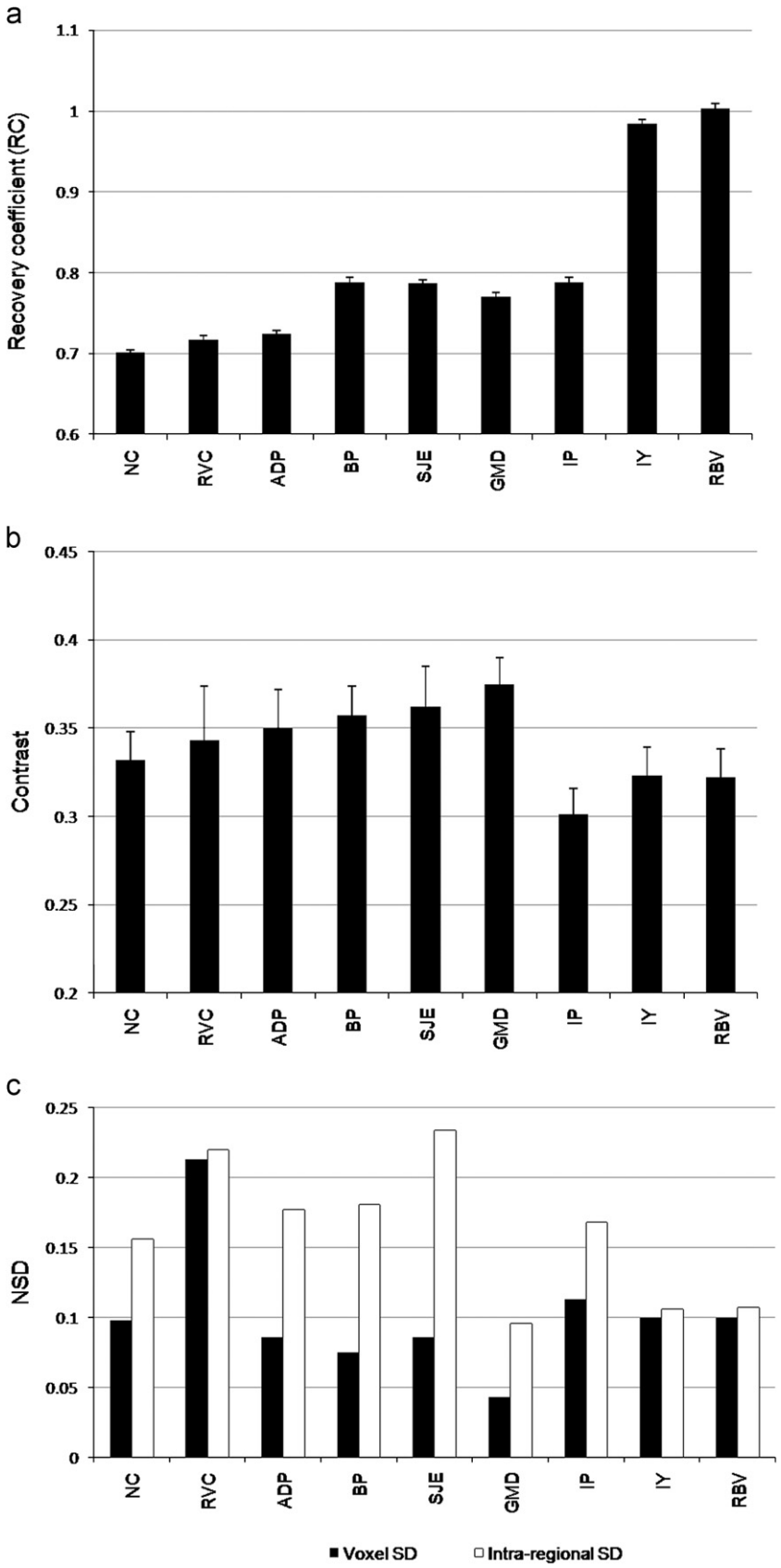

Fig. 2. Analysis results for ^{18}F–FDG using various PV correction methods. Refer to text and legend of Fig. 1 for definition of abbreviations. (a) Recovery coefficient (RC) for temporal lobe; (b) contrast for lesion absent from MRI; and (c) normalised standard deviation as a measure of variability across noise realisations (voxel SD) and uniformity (intra-regional SD).

2.3. Data analysis

The recovery coefficient (RC) was estimated as the 5% trimmed mean value within each of the defined regions (uniform and heterogeneous). In addition the recovery was measured for specific lesions. Noise was recorded as the mean normalised standard deviation (NSD) across individual pixels within specific regions for the 10 noise realisations. In addition, uniformity within reconstructed regions was assessed using the intra-regional variance (minus pixel variance). A mis-registration of the MRI data and segmented regions by 1.4 mm was also assessed.

3. Results

Representative FDG images are presented in Fig. 1(b). These demonstrate visually the superiority of methods that utilise MRI information, especially BP and SJE. FDG results for a single brain region (right temporal) and a 1 cm diameter, 50% contrast hypointense lesion are presented in Fig. 2. Cortical recovery is the best for IY and RBV (not surprising given ideal segmentation), but these display poor performance for the lesion as it is not present in the parcellation. Several of the reconstruction methods (ADP, BP, SJE) have limited cortical recovery but perform well for the lesion and have good noise properties. GMD performs similar to reconstruction methods both in preserving lesion contrast and controlling noise. Amyloid tracer (AT) recovery (right temporal) is presented in Fig. 3. The lower contrast between grey matter and white matter for the AT appears to result in larger biases, particularly for RVC and IP. Results of mis-registration of the MRI by 1.4 mm are presented in Fig. 4. RBV and IY are sensitive to mis-registration whereas other techniques are more tolerant.

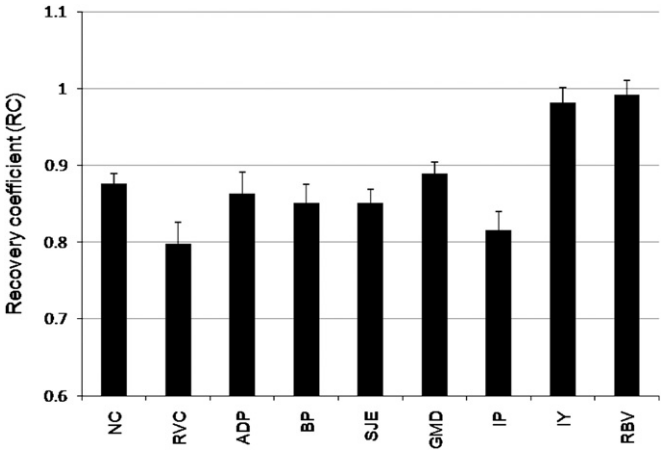

Fig. 3. Recovery coefficient (RC) for amyloid tracer in the temporal lobe using the various PV correction methods. Refer to text and legend of Fig. 1 for definition of abbreviations.

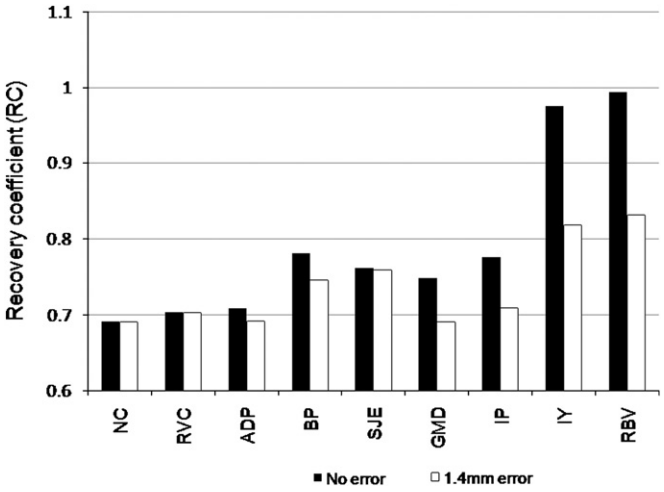

Fig. 4. Effect of registration error on the recovery coefficient for ^{18}F–FDG in the temporal lobe using high count data. Mis-registration of 1.4 mm (1 pixel in x and z) was applied to the original MRI and segmented template.

4. Discussion

This paper provides a preliminary evaluation of a range of potential PV correction techniques, with specific interest in what may be the recommended approach for simultaneous PET/MRI. The findings suggest that the various methods offer different benefits and so may be best suited to specific tasks. In particular, reconstruction methods incorporating priors provide good preservation of lesion contrast (even when absent from MRI) whereas post-reconstruction methods reduce bias in regional quantification, but require accurate segmentation and registration.

It is important to highlight some limitations in the current study design which will be rectified in future work. We used segmented MRI data to generate the Monte Carlo activity distribution, with constant activity in most of the parcellated regions. Although we did evaluate mis-registered MRI, our reference estimates used the same set of segmented regions for PV correction as used for phantom production. Our results therefore reflect an over-ideal situation where segmentation is correct in identifying regions that can be considered uniform. In practice there will be inexact segmentation and no guarantee regarding activity uniformity. To further illustrate the potential for misinterpretation the modified Bowsher prior was further modified so as to adopt all neighbours in the same labelled class as that of the voxel of interest as defined by segmentation. In this preliminary study RC improved to 96% while lesion contrast was relatively unchanged. This suggests that the observed differences largely reflected differences in the prior information used rather than the algorithm adopted (post-reconstruction versus reconstruction). This clearly requires further study.

A further limitation was the somewhat naive evaluation of performance, where reconstruction parameters were selected arbitrarily to reflect the typical application of the various correction methods. Post-reconstruction methods were applied to data reconstructed with filtered back projection with a 4 mm Gaussian filter. Variation of filter parameters would result in a change in both noise level and reconstructed resolution, necessitating adjustment of the point spread function used in the correction algorithms. Similarly the reconstruction based methods all require choice of hyper-parameters that control the influence of the anatomical prior, which would directly affect both noise and recovery. A more complete evaluation will require construction of bias-noise plots that reflect performance for a range of selected hyper-parameters. This will be the subject of future investigation.

Several of the techniques described are relatively new and warrant further discussion. The iterative Yang correction is very attractive as it is efficient and a relatively simple technique; it provided excellent recovery, similar to that of RBV. The modified Bowsher prior reconstruction was visually appealing and had good noise properties and lesion contrast. It is based on a relatively simple intuitive approach, adapted from the original published algorithm, which works surprisingly well. Both GMD and SJE make use of hidden Markov random fields to describe the underlying tissue (classes) common to both MRI and PET, although this information is used in different ways in

post-reconstruction deconvolution (GMD) and reconstruction (SJE). There is scope for both techniques to be further developed and more fully evaluated.

5. Conclusion

Overall no single PV correction technique proved better than the others, although RBV and IY had the best cortical recovery when able to utilise ideal segmentation. Results were, however, quite sensitive to mis-registration. Reconstruction-based methods and GMD outperformed RBV and IY for lesion contrast with BP and GMD having particularly good noise characteristics. The study highlighted not only the importance of accurate segmentation in achieving optimal recovery, but also the importance of adopting an appropriate prior model. It also demonstrated the potential of newer algorithms that adopt a more complete probabilistic model of the dual imaging modalities.

Choice of PV correction method is likely to depend on application (e.g. detection of lesions as opposed to regional cortical quantification). The availability of simultaneous PET/MRI, ensuring optimal registration, reduces concern regarding mis-registration and should encourage wider adoption of PV correction algorithms for routine use.

Acknowledgements

AB, DK and SP acknowledge support from the EPSRC (EP/G026483/10) and KE from EPSRC/CRUK (C1519/A10331). KV was in receipt of a visiting researcher scholarship supported by KUL and COST TD1007. UCL and UCLH receive a portion of their research funding from the UK Department of Health Biomedical Research Centres funding scheme.

References

[1] K. Erlandsson, I. Buvat, P.H. Pretorius, B. Thomas, B.F. Hutton, Physics in Medicine and Biology, in press.
[2] A. Reilhac, C. Lartizien, N. Costes, S. Sans, C. Comtat, R.N. Gunn, A.C. Evans, IEEE Transactions on Nuclear Science NS-51 (2004) 46–52.
[3] B.A. Thomas, K. Erlandsson, M. Modat, L. Thurfjell, S. Ourselin, B.F. Hutton, European Journal of Nuclear Medicine and Molecular Imaging 38 (2011) 1104–1119.
[4] O.G. Rousset, Y. Ma, A.C. Evans, Journal of Nuclear Medicine 39 (1998) 904–911.
[5] J. Yang, S.C. Huang, M. Mega, K.P. Lin, A.W. Toga, G.W. Small, M.E. Phelps, IEEE Transactions on Nuclear Science NS-43 (1996) 3322–3327.
[6] K. Erlandsson, B.A. Thomas, J. Dickson, B.F. Hutton, Nuclear Instruments and Methods in Physics Research A 648 (2011) S85–S88.
[7] A. Bousse, S. Pedemonte, K. Erlandsson, B.A. Thomas, S. Ourselin, S. Arridge, B.F. Hutton, IEEE Nuclear Science and Medical Imaging Conference Record, 2012, to appear.
[8] J. Tohka, A. Reilhac, NeuroImage 39 (2008) 1570–1584.
[9] K. Vunckx, A. Atre, K. Baete, et al., IEEE Transactions on Medical Imaging 31 (2012) 599–612.
[10] D. Kazantsev, S.R. Arridge, S. Pedemonte, A. Bousse, K. Erlandsson, B.F. Hutton, S. Ourselin, Physics in Medicine and Biology 57 (2012) 3793–3810.
[11] S. Pedemonte, M.J. Cardoso, A. Bousse, et al., Class conditional entropic prior for MRI enhanced SPECT reconstruction, in: IEEE Nuclear Science Symposium of Medical Imaging Conference Record, 2010, pp. 3292–3300.